Sensors and Actuators A 285 (2019) 386–394

Contents lists available at ScienceDirect

Sensors and Actuators A: Physical

journal homepage: www.elsevier.com/locate/sna

A compact wireless power transfer system at 915 MHz with supercapacitor for optogenetics applications

Le-Giang Tran [a], Hyouk-Kyu Cha [b], Woo-Tae Park [a,c,*]

[a] Convergence Institute of Biomedical Engineering and Biomaterials, Seoul National University of Science and Technology, South Korea
[b] Department of Electrical and Information Engineering, Seoul National University of Science and Technology, South Korea
[c] Department of Mechanical Engineering, Seoul National University of Science and Technology, South Korea

ARTICLE INFO

Article history:
Received 24 August 2018
Received in revised form 25 October 2018
Accepted 19 November 2018
Available online 20 November 2018

Keywords:
Wireless power transfer
Optogenetics
Bioimplantable
Supercapacitor
Voltage multiplier

ABSTRACT

To facilitate sophisticated optogenetics research with minimal disruption to animal's behavior, a fully wireless optical stimulator module is desirable. This paper presents a compact wireless power transfer (WPT) system for optogenetics applications that is adapted to work in implanted condition with unstable and insufficient ambient RF energy field. The scope of this work is to design and implement a power transfer system architecture that is able to: 1) work over long distance, 2) achieve high power conversion efficiency and 3) provide stable output power for sufficient time duration. The designed WPT circuit operates at 915 MHz and achieves maximum power conversion efficiency of 50% at −15 dBm input power. With a compact circuitry design (12.20 × 13.22 mm), the obtained full power transmission efficiency was 0.329% at 20 dBm (100 mW) transmission power. Ex-vivo experiments indicated that when the WPT system was located 10 cm from the source, it retrieved a maximum of 0.324 mW in free space, and 0.112 mW if inserted inside porcine cadaver meat with 4 cm of thickness. At a distance of 1 m from the source, the system retrieved 17 μW in free space, and 1 μW in porcine meat. Furthermore, to sufficiently drive the LED, an advanced supercapacitor was utilized as an energy storage element. When fully charged, the system can supply the LED over 75 s with a total power of 2.45 W. The developed WPT system can be a viable solution to be applied in optogenetic experiments on laboratory animals for preclinical studies.

1. Introduction

Wireless power transfer (WPT) technology provides seamless power to drive low-power circuits and systems in scenarios such as implantable devices where the periodic replacement of batteries is difficult and the space is limited. A WPT system uses electromagnetic waves at radio frequency (RF) to transfer energy through space. The first demonstration of the WPT was performed in the 1950s with a microwave-powered helicopter system [1]. Until recently, wireless power harvesting or transferring are conceptualized as a system that reap the energy in the surrounding environment (solar, thermal, vibration, etc.) and converts it into usable electrical energy.

Electromagnetic wave with frequency at UHF band (spreading from 300 MHz to 3 GHz) is widely used for communications and in short range energy transfer. RF power transfer is suitable to power a few μW to less than 1 mW of power. Since the total efficiency of the entire WPT system mainly depends on the performance of the receiver module [2], many researchers focused on developing high performance receiver modules. Song et al. designed broadband high sensitivity antenna (-35 dBm) for energy harvesting [3]. Moreover, antennas with optimized efficiency to minimize energy leakage were introduced in [4–6]. Others worked on the optimization of the voltage multiplier [7–10]. Furthermore, thanks to the development of MEMS technology, low-power sensors and devices are now available and can be integrated with RF power transfer chain for sustainable operation. Table 1 lists some prospective system-on-chip (SoC) sensors that consume less than or around 1 mW which can be integrated with a WPT system. These SoCs can fully operate in wireless setting with the help of WPT technology.

RF electromagnetic wave was demonstrated to be capable of efficiently transferring energy through human tissue in many literatures [11,12]. There are also researches and demonstrations which assert the benefit of RF power transfer over conventional batteries

Abbreviations: WPT, wireless power transfer; RF, radio frequency; UHF, ultra high frequency; SoC, system-on-chip; PCE, power conversion efficiency; IMN, impedance matching network; EEG, electroencephalography; ECG, Electrocardiography.

* Corresponding author. Present address: Room 301, Dasan Hall, 232 Gongneung-ro, Nowon-gu, Seoul, 01811, South Korea.
E-mail address: wtpark@seoultech.ac.kr (W.-T. Park).

https://doi.org/10.1016/j.sna.2018.11.029
0924-4247/

Table 1
Published biosensor SOC devices with low power consumption.

Refs.	Embedded sensors	Minimum operation voltage (V)	Power consumption (μW)	Size (mm)
[46]	3-channel ECG, bio-impedance	1.2	345	7 × 7
[47]	ECG, EMG, EEG	0.3	19	2.5 × 3.3
[48]	3-channel ECG, electrode-tissue-impedance	1.2	32	5 × 4.7
[49]	Thoracic impedance variance (TIV), ECG	1.2	3900	5 × 5
[50]	64-channel Electrocorticography (ECoG)	–	225	2.4 × 2.4
[51]	Piezoelectric sound sensor	1.5	10.25	3.6 × 3.6

[13,14]. Others tried to utilize WPT technology to provide seamless access to deep brain stimulation device [15], neurorecording device [16], and optofluidic neural probe [17]. The aforementioned work operated in the distance less than 20 cm from the source. As the operation distance of the WPT system is improved, it would provide the testing subject with more mobility.

Optogenetics is an integration of genetics and optical technology to precisely control the activity of a specific cell in living tissue [18] which is a new approach to investigate neurological disorders [19]. This method is a branch of neuroscience in which using optical signal as stimulus to gain or lose some well-defined functions of targeted cells. Gradinaru et al. applied optogenetics to interpret the effects of deep brain stimulation device on Parkinson's disease [20]. Thus, the current developments of optogenetics combined with advanced WPT technology are imperative to be realized for medical applications.

In optogenetics, the input optical stimulus is generated by a light source (e.g. LED) that emits the appropriate light beam. Once the subject is triggered by optical stimulus, the behavior of the subject changes according to functions of the triggered cell. The subject's behavior is recorded for further analysis [21]. Therefore, experiment setup uniquely requires the subject (usually mice) to freely move in an enclosed space. The ideal solution for this condition is to have a small size wireless optogenetic device. As reported in [22], a wireless powered optogenetic microneedle was fabricated and tested in mice. The WPT system in this previous work was able to produce 4.08 mW of electrical power from a 7.9 W source at a distance of 1 m. Despite the reported low efficiency, the system sufficiently supported the optogenetic microneedle while providing the mice freedom in movement. However, this work encountered unstable working condition due to the disturbance of input energy while the mice was moving.

In terms of light intensity, optogenetics requires lower light intensity than typical display applications. Channelrhodopsin (ChR2) and halorhodopsin (VChR1) cells can be activated by a light intensity of 1.2 mW/mm^2 for 406 nm wavelength or 2.3 mW/mm^2 for 589 nm wavelength [23]. And for safety considerations, light intensity be should always less than 100 mW/mm^2 to prevent tissue damage [24]. Recently, the development of micro-LED technology allowed fabrications of ultra-low power consumption LEDs. For example, the flexible vertical micro-light-emitting diodes (f-VLED) induced light intensity of 2.7 mW/mm^2 at 0.8 mW input power, which is sufficient for optogenetic applications [25]. The micro-LED presented by Wu et al. induced light intensity of 67 mW/mm^2 at 0.114 mW input power [26]. The micro-LED technology is a promising illumination solution for optogenetics because of their small size, high efficiency and low-power consumption.

This paper presents the design of a long-range, highly efficient RF power transfer system targeting low-power implanted LED for optogenetics applications. An RF WPT receiving module is proposed which harnesses electromagnetic waves at 915 MHz to transfer energy over the distance of 1 m. The novelty of this work lies on the long working distance with high power transfer efficiency even in an energy insufficient zone. This work targets applications such as optogenetics that require around 1 mW of electrical power. Using WPT, the physical boundary can be eliminated, allowing the experiment subjects to have freedom in movement. The system is expected to eliminate geographical boundary for applications such as health indexes monitoring and support treatments for chronic diseases.

Regarding the safety issue, the specific absorption rate (SAR) of RF transmitter must be controlled. According to the Federal Communication Commission (FCC) for transmitter using external antennas for indoor or outdoor operation must have output power lower or equal to 2.5 W at 915 MHz to ensure compliance for spread spectrum transmitters [27]. In this work, we utilized the 915 MHz electromagnetic wave, which is generated by a RF signal generator connected to a panel antenna. Since the maximum generated power was 0.1 W at 915 MHz, due to device limit, which is 25 times lower than the FCC regulation, we considered the SAR level in the experiment area was lower than the limits.

The article is organized as follows. Section II discusses the overall WPT system architecture and general design considerations. Section III narrates the essential steps and method to design a WPT system. Section IV describes the experiments to verify the performance of the WPT circuit in different conditions. This section also covers the discussion following each experiment result. A brief conclusion notice is given in Section V.

2. Wireless power transfer design architecture and general considerations

The block diagram of the WPT system is depicted in Fig. 1. The RF power generator is used to produce a RF signal at 915 MHz with a magnitude of + 20 dBm. The following 12.5 dBi gain panel antenna emits RF waves in the horizontal direction. The receiving module starts with the antenna connected with an impedance matching network. This is followed by a rectifier/voltage multiplier, a power management unit, an energy storage element and an output load. The impedance matching network ensures maximum power transmission from the receiving antenna to the rectifier/voltage multiplier and the load. The rectifier converts the RF signal into DC voltage. Converted DC voltage is also amplified if the voltage multiplier is used instead of the rectifier. The power management module in this work is used to provide a stable current to charge the supercapacitor and drive the load.

In order to efficiently frame the challenges to design the WPT circuit, it is critical to understand the electromagnetic conditions of the environment which the circuit is working in before designing the electrical parts. The electromagnetic wave is comprised of the electric field and magnetic field components. As the electromagnetic wave propagates in space, the magnitude of the electric and magnetic field fluctuates at a certain frequency. The region of the electromagnetic wave is classified into the near-field and far-field. In the near-field, the electric and magnetic field exits independently. However, in the far-field, the two components oscillate in phase. These two fields are separated by a value called the Fraunhofer's distance, which is defined as:

$$d_f = 2D^2/\lambda \quad (1)$$

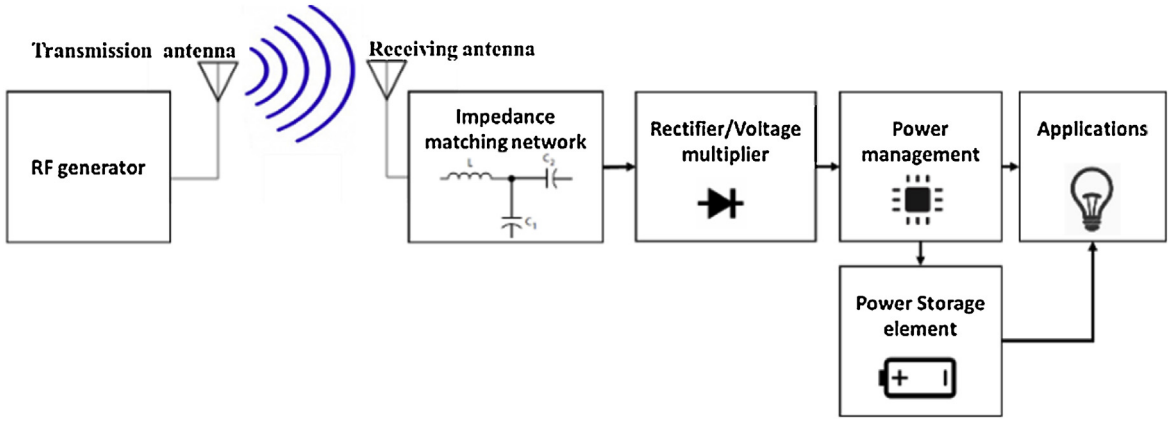

Fig. 1. Block diagram of the wireless power transfer system.

Table 2
Designed parameters of the WPT transmission conditions.

Transmitter	Symbol	Unit	Value
Transmitted power	P_T	dBm	20
Transmitter antenna gain	G_T	dBi	12.5
Transmitter feeding loss	G_{Tf}	dB	0
Frequency	f	MHz	915
Receiver			
Receiver antenna gain	G_R	dBi	−2
Receiver mismatch loss	G_{Gf}	dB	0
Wave propagation			
Distance	D	m	1
Free space loss	P_L	dB	31.7
Air propagation loss	P_a	dB	0
Received power	P_R	dBm	−1.2

where D is the largest dimension of the radiator (in this case the diameter of the antenna) and λ is the wavelength of the electromagnetic wave. λ

In this work, the D value of the transmitter panel antenna was 0.55 m. Thus, from (1), the calculated d_f is 1.84 m at 915 MHz. Since the targeted operation range of the WPT system was 1 m from the source, this work deals with the near-field of the electromagnetic waves.

The free space path loss P_L is calculated as follows:

$$P_L = 10\log_{10}\left(4\pi d/\lambda\right)^2 \quad (2)$$

where d is the distance between the transmitter and receiver.

Assuming the ideal condition with the transmission and receiving was as provided in Table 2, the received power P_R can be calculated from the formula adopted from [28]:

$$P_R = P_T + G_T - G_{Tf} + G_R - G_{Gf} - P_L - P_a \quad (3)$$

As the path loss P_L is a function of distance, the received power was computed as a function of distance as shown in Fig. 2. Notice that P_R is the power received by the receiver antenna, the real power delivered to the load is always less than P_R.

The received power at the antenna drops rapidly as the distance between the transmitter and receiver increases. At 1 m distance from the transmitter source, the received power was -1.17 dB m (~0.76 mW). It is inferred from Fig. 2 that the WPT circuit will work with very low power (< 1 mW). Therefore, a voltage multiplier rather than a rectifier should be used in order to provide a suitable level of voltage.

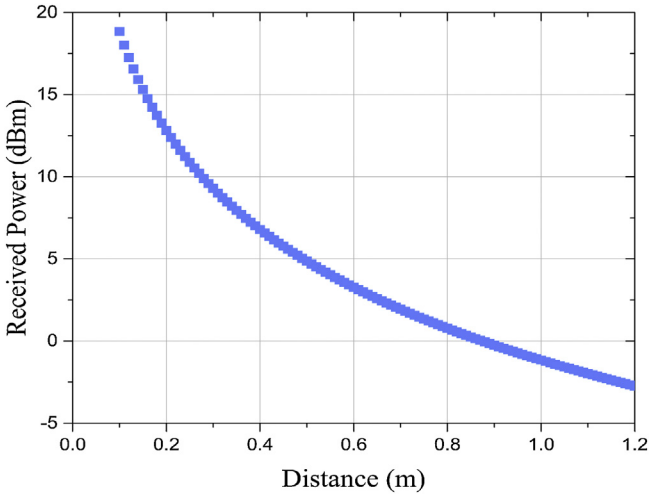

Fig. 2. The degrading of the received power to distance.

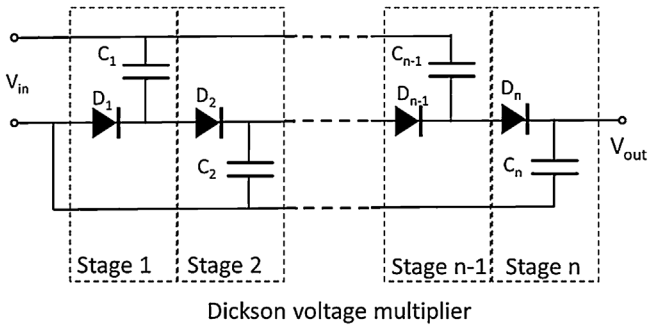

Fig. 3. Schematic diagram of Dickson voltage multiplier.

3. Wireless power transfer system design

3.1. Voltage multiplier

The voltage multiplier is a critical module in the WPT system which boosts the output voltage to sufficiently drive the application. By connecting multiple rectifier circuits in series, the voltage builds up after each rectifier stage [29]. Adding more stages in the voltage multiplier would increase the output voltage. On the contrary, due to the diode voltage drop, adding more stages lead to degradation in efficiency. Thus, there is a tradeoff between amplified output voltage and power conversion efficiency (PCE). This

tradeoff feature was discussed in some studies [8,30]. For a high *PCE* circuit, it is recommended to design a 3–5 stages voltage multiplier, while the higher number of stages retrieves more sustainable output.

In this work, the Dickson configuration is employed in the voltage multiplier design. In Dickson configuration, the stage capacitors are shunted to eliminate parasitic effects. These features are important for low-power circuit. The schematic of the Dickson voltage multiplier is depicted in Fig. 3. At the first half cycle, capacitor C_1 is charged through diode D_1 to a voltage level that equals to V_{in}. In the next half cycle, capacitor C_2 is charged through diode D_2 to a voltage level which is a sum of V_{in} and the charged voltage at C_1 (which results in twice the value of V_{in}). Therefore, the voltage across C_2 is doubled in comparison with V_{in}. Consequently, the voltage across C_n is $n \times V_{in}$, theoretically.

In order to evaluate the performance of the voltage multiplier, we analyzed the output voltage and PCE. The PCE is calculated from the following formula:

$$\eta_e = P_{DC}/P_{in} = (V_{DC}^2/R_L).(1/P_{in}) \quad (4)$$

where P_{DC} is the output measured power consumed by the load resistor R_L, and P_{in} is the input RF power to the rectifier.

The rectifying element was the main factor that dictated the PCE of the voltage multiplier. As we work in the with the low-power condition, we selected the Schottky diode (HSMS 2850) for the voltage multiplier. HSMS 2850 has high signal sensitivity up to 50 mV/μW at 915 MHz. Since the application required a supply voltage slightly greater than the forward voltage of the LED only, we tried to implement the least number of multiplying stages. Minimizing the number of stages of the voltage multiplier not only improved the PCE but also reduced the circuit size and weight. In addition to the PCE value, the power transmission efficiency (PTE), which is the ratio between the receiving power over the transmitting power in percentage [31], was also used to evaluate the performance of the system. The PTE value counted include the free space loss, PCE of the circuit and antenna gain, therefore, provides a general parameter to compare a wireless power transferring system.

3.2. Impedance matching network

Ensuring maximum power to be transferred from the receiving antenna to the load is important since the amount of power is limited. At μW power level, every bit of energy is counted for the total efficiency of the system. The impedance matching network (IMN) was used to improve the efficiency of transmission in the circuit.

It is well known in DC circuits that transmission loss in the circuit is minimized when resistance of the source and load are identical. Thus, the IMN is added in-between the receiving antenna and the voltage multiplier to match the impedance of the two blocks. The IMN comprises of inductors and capacitors. In this work, we designed the IMN following the T and π network as previously reported in [32]. Lump components were used to build the IMN. The resonance frequency of the matching was tuned at 915 MHz.

3.3. Power management and supercapacitor

In scenarios where available RF source is insufficient for the application, the power transferring system may not be able to provide sufficient power to the load. As the incident RF power is low,

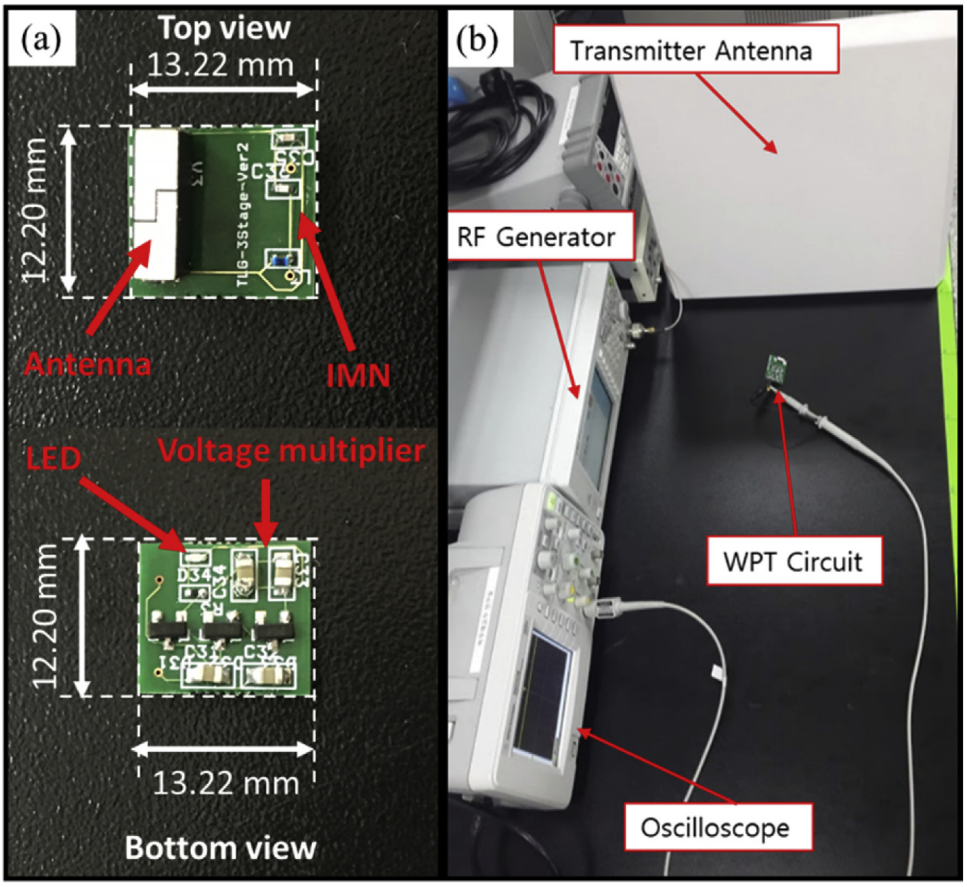

Fig. 4. Photo of the WPT circuit (a) and basic experiment setup (b). The RF generator was directly connected to the panel antenna via a SMA cable. Oscilloscope was used to measure the output voltage (a multimeter was alternatively used sometime).

Table 3
Comparison with state-of-the-art works.

References	[31]	[33]	[44]	[45]	This work
Technology	RF radiation	RF radiation	RF radiation	RF radiation	RF radiation
Frequency	433 MHz	2.51 GHz	2.4 GHz	915 MHz	915 MHz
Receiving antenna area	100 mm^2	24 mm^2	Whip type	546 mm^2	57.6 mm^2
Transmitting power	25.1 W	0.27 W	0.02 W	3 W	0.1 W
Max *PCE*	86% @ 11 dBm	NA	34.7% @ 0 dB m	78% @ -5 dBm	50% @ -15 dBm
Max PTE	0.04% (minced pork)	0.157% @ 0.3 m (minced pork)	0.885×10^{-6} % @ 0.01 m	0.337% @ 0.1 m (free space)	0.329% (free space), 0.11% (porcine meat) @ 0.1 m
Max output power	10.86 mW @ 0.5 m, 44 dB m input	0.424 mW @ 0.3 m, 24.3 dB m input	1.77×10^{-10} W	10.1 mW @ 0.01 m (free space)	0.329 mW (free space), 0.11 mW (porcine meat) @ 0.1 m, 20 dB m input
Application	Implanting	NA	Charging of mobile devices	Deep brain simulation	Optogenetic

the voltage multiplier may not provide enough voltage to drive the LED. Furthermore, the WPT receiver can be as far as 1 m from the RF source and implanted under the skin, thus, the received power is expected to be unstable and low. To address this challenge, many other works tried to increase the RF radiation power so receiver ca retrieve more power [33–35]. However, the RF power density degrade drastically as it is moving away from the source. To overcome this challenge, a power management system with a supercapacitor as an energy storage element was implemented. The expected outcome is improvement in delivering more stable current. While the WPT receiver circuit retrieves RF energy, the supercapacitor is steadily being charged. The LED draws power from the supercapacitor, so the system can work even in insufficient RF power transmission.

The supercapacitor offers quick charging, unlimited cycle time, and much smaller in size than conventional LiPo and NiMH batteries. The power-to-weight ratio of supercapacitor is up to 10,000 W/kg while it is around 3000 W/kg for LiPo batteries and around 1000 W/kg for NiMH batteries [36]. The charging/discharging time of super capacitor is 360 times faster than lead acid battery [37]. Supercapacitors can have more than 1×10^5 recharge cycles, which is 100 times higher than Li-ion batteries [38]. Supercapacitors are also suitable for peak power and short-term storage applications [39]. In this work, we implement the BQ25570 power management IC (Texas Instruments) with 100 m F supercapacitor. The limit voltage of this supercapacitor was 5.5 V, which was capable of storing 1.5 J energy when fully charged.

4. Experiments and results

Fig. 4(a) shows the implemented WPT circuit with 3-stage voltage multiplier designed on the 2-layer custom printed circuit board. On the top layer, the receiving antenna and IMN is placed while the voltage multiplier and LED were implemented on the bottom layer.

In the experiment section, in order to collect reliable and interpretable data, we utilized different versions of the voltage multiplier for each experiment based on the nature of the experiment. In the experiment to electrically characterize the performance of the voltage multiplier and the power management unit with the supercapacitor, we used the simple 3-stage voltage multiplier.

In the wireless experiments, additional number of stages for the voltage multiplier was used. To resemble the porcine skin implanting scheme, a thick porcine meat blocks the RF waves, thus, the receiving module only received a limited amount of energy. Therefore, we used higher number of stages for the voltage multiplier to boost the DC voltage. Furthermore, the output voltage is more stable at high stages voltage multiplier. Higher number of stages for the voltage multiplier was used also in the experiment with the LED.

4.1. Voltage multiplier characterization

The experiment was setup as shown in Fig. 4(b). In this experiment, the RF signal generator was Keysight N9310 A RF. The transmitting antenna was a panel antenna ARC-PCA0913B01 (ARC Wireless LLC), 902–928 MHz, 12.5 dBi. The panel antenna was directly connected to the output of the RF signal generator. For the receiving antenna, we used the W3012 ceramic antenna (Pulse-Lasen Electronics), 902–928 MHz, 2 dBi. The area of the receiving antenna was 100 mm^2. To measure output voltage of the receiver module, the oscilloscope was connected in parallel with the load resistor. From this output voltage, the output power and PCE was calculated. To validate the performance of the voltage multiplier, the input power was tuned from −15 to + 20 dBm with 5 dB steps. The load resistance R_L was fixed at 10 kΩ. In addition, the 1 m space in front of the transmitting antenna was left empty with no obstacles. The WPT circuit was located in the middle of the transmitting antenna.

The advantage of the high gain antenna is that it can focus the RF wave into a single direction, thus, creating a sufficient environment of RF energy along that direction. On the other hand, if the receiving antenna was not in the main direction of the transmitting antenna, the retrieved energy was significantly reduced.

As shown in Fig. 5(a), the graph shows that the output voltage in three different versions of the rectifier/voltage multiplier are in agreement with the theory where the output voltage is a multiplication of the stages. For instance, at + 10 dBm input RF power, the 3-stage voltage multiplier produced 4.8 V while the 2-stage and single-stage full-rectifier produced 3.0 V and 1.5 V, respectively.

Even though the voltage builds up in each stage of the voltage multiplier, with the more stages added, the efficiency dropped further due to the added voltage drop in the diodes as shown in Fig. 5(b). On the other hand, addition of further stages helped stabilize the output voltage since capacitors in each stage worked as local storage of energy. Therefore, for wireless application where incident power is unstable and random, multiple stages of voltage multiplier is preferred.

Another parameter to evaluate the performance of the voltage multiplier is the PCE: η_e. The η_e of the circuit is calculated as (4). As shown in Fig. 5(c), the maximum PCE achieved by the 3-stage voltage multiplier is 50% at −15 dBm input power. As the input power increases, the transfer voltage and delivered power increases while the overall PCE decreases. It is apparent from the graph that the PCE is inversely proportional to the input RF power. Z. Hameed et al. reported maximum PCE of 22.6% and they also recorded the unpredictable variation of the PCE to the input power [40]. In comparison with inductive coupling power transfer, the RF radiative power transfer had lower PCE and PTE but the trade-off was longer

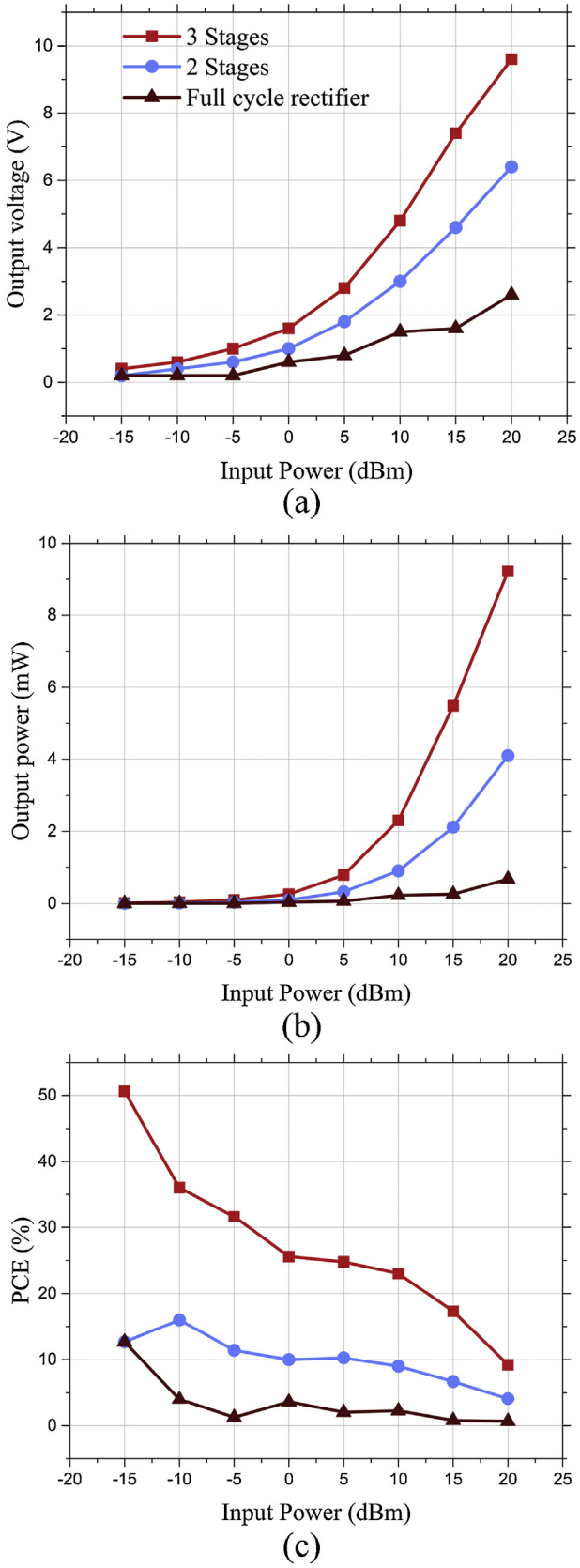

Fig. 5. Output voltage, power and PCE of the three versions of the rectifier/voltage multiplier circuit. (a) The output voltage measured across the load resistance versus input RF power. From the output voltage, the calculated power (b) and PCE (c) are shown.

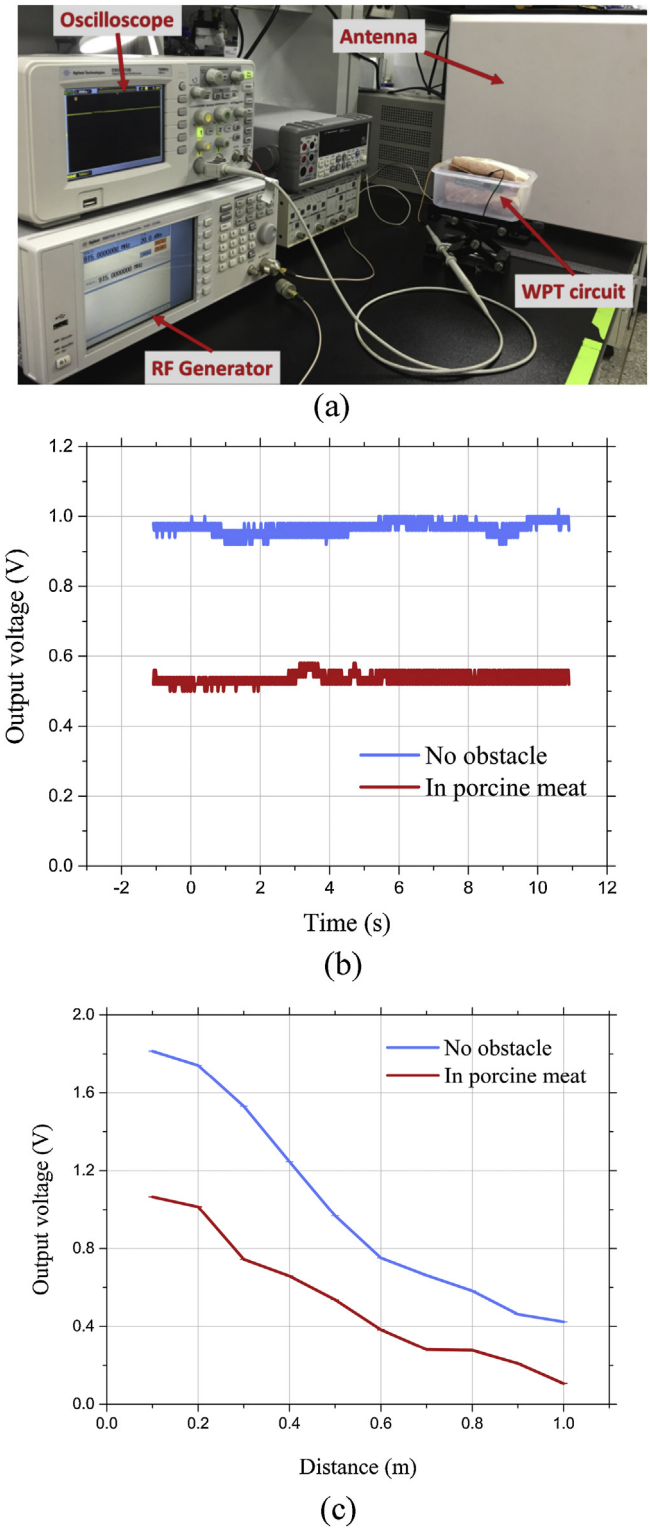

Fig. 6. (a) Setup of the measurement of the WPT performance in porcine cadaver meat. (b) The oscilloscope output of the WPT circuit at distance 0.5 m from the transmitting antenna. (c) Graph showing the output voltage received at different distances.

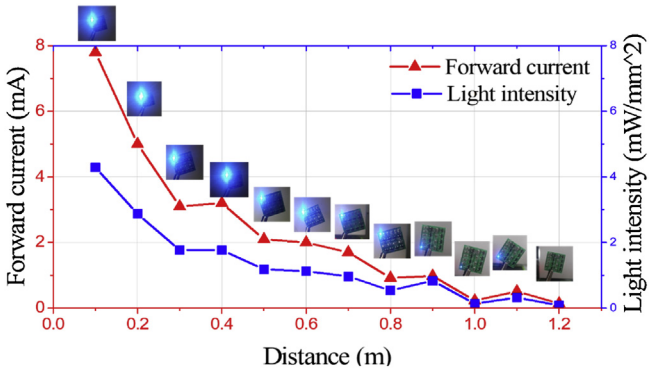

Fig. 7. Characteristic of the WPT with distance. The brightness of the LED was captured and displayed with the corresponding calculated light intensity. The 8 stages Dickson voltage multiplier was used in this experiment. The input power from the RF generator to the transmitting antenna was 25 W.

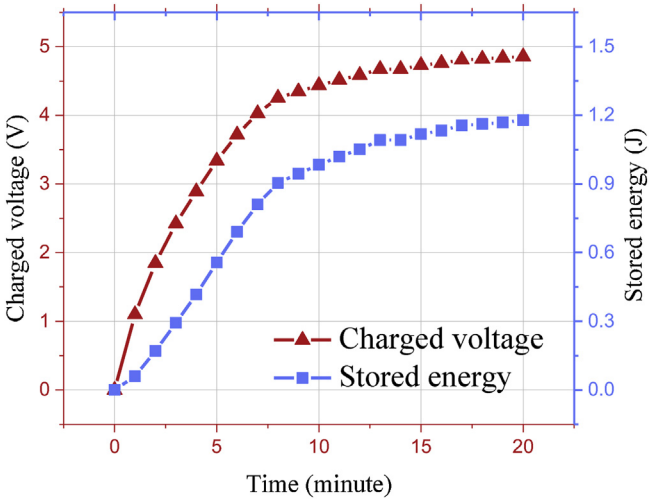

Fig. 8. Charging the supercapacitor at 20 dB m incident RF power input. The 3 stages voltage multiplier was used to boost the charging unit.

operation distance [41–43]. Table 3 provides the comparison of the PCE with other literatures.

4.2. Measurement in porcine meat

The whole WPT circuit was attached to the back side of a 4 cm thick porcine cadaver meat which is depicted in Fig. 6(a). This setup resembles the actual implant condition in human body where the WPT module is inserted under the skin. In this experiment, transmitting RF power was + 20 dBm at 915 MHz, and output voltage was measured through a 10 kΩ load resistor. A 15-stage voltage multiplier was used in this experiment. As shown in Fig. 6(b), the observed output voltage was stable over time. When the circuit was inserted behind the porcine meat, the received voltage dropped by almost 50% in comparison to the condition in free space (Fig. 6(c)). The average output voltage of the measurement in porcine meat at 0.5 m distance was 0.54 V while without meat is 0.97 V. As would be expected, the porcine meat attenuated considerable amount of RF energy. At a distance of 0.1 m from the transmitting antenna and inserted behind the porcine meat, the WPT circuit retrieved 1.07 V, corresponding to 0.11 mW power. Considering the operation voltage and power consumption of the sensors reported in Table 1, the proposed WPT circuits can possibly support most of the listed sensors at distance from 10 cm to 50 cm from the source.

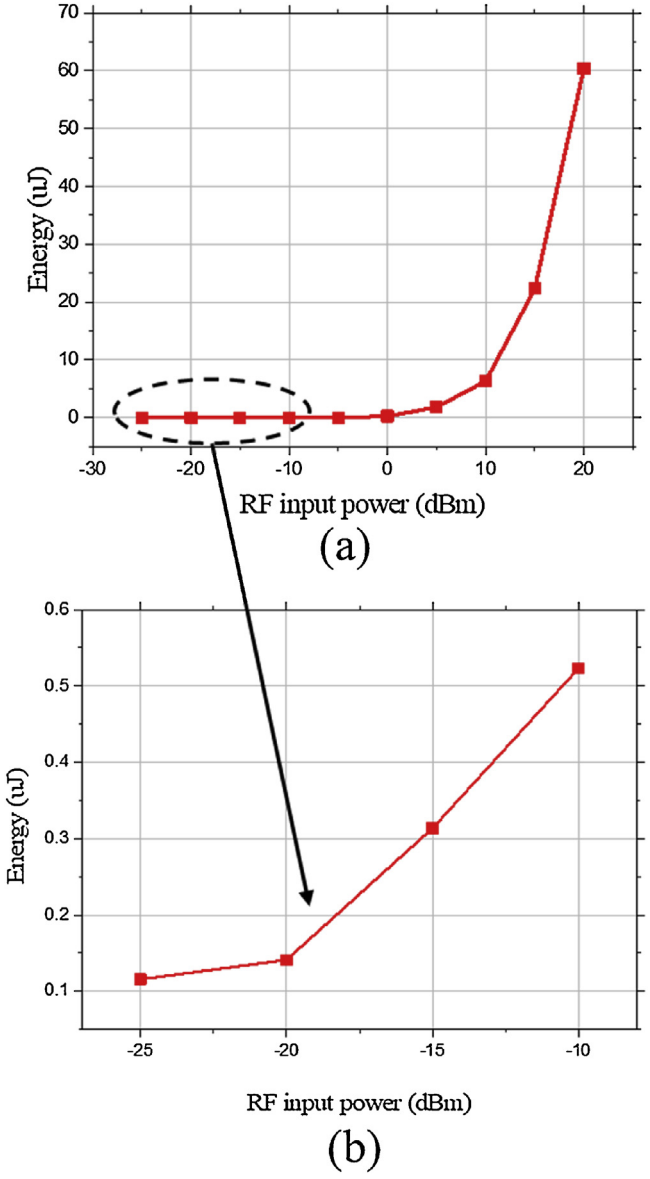

Fig. 9. Energy charged in 1 min with different incident RF input power. Data measured on the 3 stages Dickson voltage multiplier.

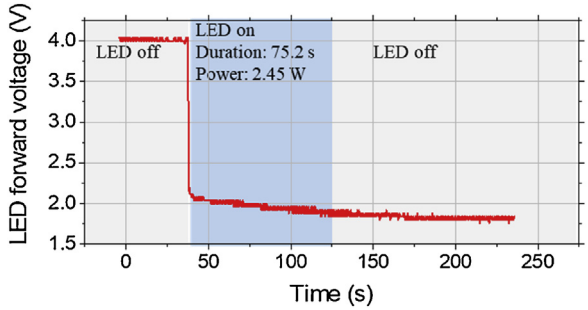

Fig. 10. Forward voltage of the LED. The circuit was charged to 4 V in the supper capacitor, it was capable to drive a LED for 75.2 s.

A comparison of the PCE and PTE is shown in Table 3. There were two cases: The maximum PTE in reached 0.329% in free space and 0.11% in 4 cm of porcine meat and skin. The low PTE was expected as the RF wave propagates in the atmosphere and penetrates through 4 cm of tissues. Notice that even with the lower PCE, this work

archived good PTE in comparison with other literature in Table 3. One explanation for this is that the receiver usually works at the low RF power conditions, therefore, a system with high PCE at low input power would probably produces higher PTE. Conventionally, reducing of the receiving antenna size and transmitting power can likely lower the PTE of the system [33,44]. On the contrary, the achieved PTE of this work was similar to the system presented by Hosen et al. [45] while utilizing thirty-fold less transmitting power. The receiving antenna size reported in this work were smaller than in other relative literatures [31,44,45] while still reached similar or even higher PTE.

4.3. Powering the LED for optogenetics application

The retrieved energy was directly supplied to an LED for optogenetics application. No obstacles were placed in between the transmiter antenna and the WPT circuit. By measuring the forward current across the LED and comparing it with the bias current provided in the datasheet, we evaluated whether the WPT circuit supply suffcient power to the LED or not. Data showed that the LED was powered at the distance 0.8 m from the transmiter antenna (Fig. 7).

To better supply the LED for optogenetics application, a supercapacitor was added as an energy storage element. In this experiment, the 100 m F, 5.5 V supercapacitor was used. The input of the IMN was supplied by + 20 dBm RF power while the charged voltage and energy across the supercapacitor were recorded and calculated respectively (Fig. 8). After 5 min, the supercapacitor was charged to 3.3 V (corresponding to 60% of fully charged), and reached 4.0 V, 72% charged in 7 min.

Considering the in-vivo applications, in scenario when the incident RF power is unstable and relatively weak, the retrieved voltage and power are therefore expected to be weak. The amount of energy retrieved by the WPT in 1 min is shown in Fig. 9. From -25 dBm (3.17 μW) RF power input to the IMN, the system begins to charge the supercapacitor. At maximum + 20 dBm input power, the supercapacitor was charged to 1.1 V, corresponding to 60 mJ of energy. The energy stored in the 4 V charged 100 m F supercapacitor corresponded to 0.8 J. Data indicated that if supercapacitor is fully charged, it can supply blue LED for 75.2 s continuously (Fig. 10).

In optogenetics applications, the LED is usually used in pulse mode with frequency ranging from 3 to 20 Hz [22]. The pulse mode reduces the power consumption rate of the LED and thermal effect. Therefore, 0.8 J of energy can sufficiently supply the pulse mode LED.

The scope of this work was to design a wireless power transfer system that is able to: 1) work over long distance, 2) achieve high PCE and 3) provide stable output power for sufficient time duration. The overall performance of the system is shown in Table 3. In comparison to similar works using inductive coupling to transfer energy, the proposed system achieved lower PCE and power but was able to deliver stable power over a longer distance. Our work achieved 50% PCE at -15 dBm input power, which is an improvement over other similar works [12,44]. Because of the nature of the electromagnetic waves, the power density drops dramatically over distance, therefore, we also expected the low PCE in the ex-vivo.

5. Conclusions

In this paper, a guideline to design a WPT system specified for the target application is provided. In order to balance the parameters of the circuit, it is necessary to determine the required operating voltage, power and space. The system worked on a + 20 dBm RF supply through a 12 dBi panel antenna. Having the operation range expanded to 1 m, the system was demonstrated to successfully power the LED for optogenetics applications. Experiments with porcine meat was conducted to validate performance of the designed WPT system in in-vivo applications. Furthermore, for applications consuming less energy than the LED (around 50 μW) such as EEG, ECG, the proposed WPT system can supply the device at distances 1 m or even more from the source. Depending on the criteria of the application, the proposed WPT can be implemented to independently power the application or charge and prolong the battery life.

Acknowledgement

This work was supported by the National Research Foundation of Korea (NRF). Project # NRF-2013R1A1A1012616 & NRF-2017R1A2B4011556.

References

[1] W.C. Brown, Experiments involving a microwave beam to power and position a helicopter, IEEE Trans. Aerosp. Electron. Syst. 5 (1969) 692–702.
[2] W.C. Brown, The technology and application of free-space power transmission by microwave beam, Proc. IEEE 62 (1) (1974) 11–25.
[3] C. Song, Y. Huang, J. Zhou, J. Zhang, S. Yuan, P. Carter, A high-efficiency broadband rectenna for ambient wireless energy harvesting, IEEE Trans. Antennas Propag. 63 (8) (2015) 3486–3495.
[4] H. Sun, An enhanced rectenna using differentially-fed rectifier for wireless power transmission, IEEE Antennas Wirel. Propag. Lett. 15 (2016) 32–35.
[5] J.-H. Chou, D.-B. Lin, K.-L. Weng, H.-J. Li, All polarization receiving rectenna with harmonic rejection property for wireless power transmission, IEEE Trans. Antennas Propag. 62 (10) (2014) 5242–5249.
[6] H. Sun, Y. Guo, M. He, Z. Zhong, Design of a high-efficiency 2.45-GHz rectenna for low-input-power energy harvesting, IEEE Antennas Wirel. Propag. Lett. 11 (2012) 929–932.
[7] S.S. Chouhan, M. Nurmi, K. Halonen, Efficiency enhanced voltage multiplier circuit for RF energy harvesting, Microelectron. J. 48 (2016) 95–102.
[8] A.N. Rodriguez, F.R.G. Cruz, R.Z. Ramos, Design of 900 Mhz AC to DC converter using native Cmos device of TSMC 0.18 micron technology for RF energy harvest application, Univ. J. Electr. Electron. Eng. 3 (7) (2015).
[9] Y.-S. Hwang, C.-C. Lei, Y.-W. Yang, J.-J. Chen, C.-C. Yu, A 13.56-MHz low-voltage and low-control-loss RF-DC rectifier utilizing a reducing reverse loss technique, IEEE Trans. Power Electron. 29 (12) (2014) 6544–6554.
[10] S. Hemour, et al., Towards low-power high-efficiency RF and microwave energy harvesting, IEEE Trans. Microwave Theory Tech. 62 (4) (2014) 965–976.
[11] S.M. Asif, et al., Design and in vivo test of a batteryless and fully wireless implantable asynchronous pacing system, IEEE Trans. Biomed. Eng. 63 (5) (2016) 1070–1081.
[12] A. Abid, et al., Wireless power transfer to millimeter-sized gastrointestinal electronics validated in a swine model, Sci. Rep. 7 (2017).
[13] T. Soyata, L. Copeland, W. Heinzelman, RF energy harvesting for embedded systems: a survey of tradeoffs and methodology, IEEE Circuits Syst. Mag. 16 (1) (2016) 22–57.
[14] S. Hemour, K. Wu, Radio-frequency rectifier for electromagnetic energy harvesting: development path and future outlook, Proc. IEEE 102 (11) (2014) 1667–1691.
[15] M.K. Hosain, A.Z. Kouzani, M.F. Samad, S.J. Tye, A miniature energy harvesting rectenna for operating a head-mountable deep brain stimulation device, IEEE Access 3 (2015) 223–234.
[16] A. Kiourti, C.W.L. Lee, J. Chae, J.L. Volakis, A wireless fully passive neural recording device for unobtrusive neuropotential monitoring, IEEE Trans. Biomed. Eng. 63 (1) (2016) 131–137.
[17] J.G. McCall, et al., Preparation and implementation of optofluidic neural probes for in vivo wireless pharmacology and optogenetics, Nat. Protoc. 12 (January) (2017) 219.
[18] K. Deisseroth, Optogenetics, Nat. Methods 8 (December) (2010) 26.
[19] K.M. Tye, K. Deisseroth, Optogenetic investigation of neural circuits underlying brain disease in animal models, Nat. Rev. Neurosci. 13 (4) (2012) 251.
[20] V. Gradinaru, M. Mogri, K.R. Thompson, J.M. Henderson, K. Deisseroth, Optical deconstruction of parkinsonian neural circuitry, Science 324 (5925) (2009) 354–359 (80-.).
[21] K.L. Montgomery, et al., Wirelessly powered, fully internal optogenetics for brain, spinal and peripheral circuits in mice, Nat. Methods 12 (August) (2015) 969.
[22] T. Kim, et al., Injectable, cellular-scale optoelectronics with applications for wireless optogenetics, Science 340 (6129) (2013) 211–216 (80-.).
[23] F. Zhang, et al., Red-shifted optogenetic excitation: a tool for fast neural control derived from Volvox carteri, Nat. Neurosci. 11 (6) (2008) 631.

[24] J.A. Cardin, et al., Targeted optogenetic stimulation and recording of neurons in vivo using cell-type-specific expression of channelrhodopsin-2, Nat. Protoc. 5 (January) (2010) 247.
[25] S.H. Lee, et al., Optogenetic control of body movements via flexible vertical light-emitting diodes on brain surface, Nano Energy 44 (2018) 447–455.
[26] F. Wu, E. Stark, P.-C. Ku, K.D. Wise, G. Buzsáki, E. Yoon, Monolithically integrated μLEDs on silicon neural probes for high-resolution optogenetic studies in behaving animals, Neuron 88 (6) (2015) 1136–1148.
[27] Evaluating Compliance with FCC Guidelines for Human Exposure to Radiofrequency Electromagnetic Fields, 2018 [Online]. Available: https://www.fcc.gov/bureaus/oet/info/documents/bulletins/oet65/oet65c.doc.
[28] H. Mizuno, M. Takahashi, K. Saito, N. Haga, K. Ito, Design of a helical folded dipole antenna for biomedical implants, in: Proceedings of the 5th European Conference on Antennas and Propagation (EUCAP), 2011, pp. 3484–3487.
[29] G. Gosset, D. Flandre, Fully-automated and portable design methodology for optimal sizing of energy-efficient CMOS voltage rectifiers, IEEE J. Emerg. Sel. Top. Circuits Syst. 1 (2) (2011) 141–149.
[30] J.C.S. Kadupitiya, T.N. Abeythunga, P. Ranathunga, D.S. De Silva, Optimizing RF energy harvester design for low power applications by integrating multi stage voltage doubler on patch antenna, in: 2015 8th International Conference on Ubi-Media Computing (UMEDIA), 2015, pp. 335–338.
[31] F.-J. Huang, C.-M. Lee, C.-L. Chang, L.-K. Chen, T.-C. Yo, C.-H. Luo, Rectenna application of miniaturized implantable antenna design for triple-band biotelemetry communication, IEEE Trans. Antennas Propag. 59 (7) (2011) 2646–2653.
[32] L.-G. Tran, H.-K. Cha, W.-T. Park, RF power harvesting: a review on designing methodologies and applications, Micro Nano Syst. Lett. 5 (1) (2017) 14.
[33] C. Liu, Y.-X. Guo, H. Sun, S. Xiao, Design and safety considerations of an implantable rectenna for far-field wireless power transfer, IEEE Trans. Antennas Propag. 62 (11) (2014) 5798–5806.
[34] M. Stoopman, S. Keyrouz, H.J. Visser, K. Philips, W.A. Serdijn, Co-design of a CMOS rectifier and small loop antenna for highly sensitive RF energy harvesters, IEEE J. Solid-State Circuits 49 (3) (2014) 622–634.
[35] M. Stoopman, S. Keyrouz, H.J. Visser, K. Philips, W.A. Serdijn, A self-calibrating RF energy harvester generating 1 V at− 26.3 dBm, in: 2013 Symposium on VLSI Circuits (VLSIC), 2013, pp. C226–C227.
[36] Battery University. [Online]. Available: https://batteryuniversity.com/index.php/learn/article/whats_the_role_of_the_supercapacitor.
[37] M.E. Glavin, P.K.W. Chan, S. Armstrong, W.G. Hurley, A stand-alone photovoltaic supercapacitor battery hybrid energy storage system, in: Power Electronics and Motion Control Conference, 2008. EPE-PEMC 2008. 13th, 2008, pp. 1688–1695.
[38] H. Chen, T.N. Cong, W. Yang, C. Tan, Y. Li, Y. Ding, Progress in electrical energy storage system: a critical review, Prog. Nat. Sci. 19 (3) (2009) 291–312.
[39] X. Luo, J. Wang, M. Dooner, J. Clarke, Overview of current development in electrical energy storage technologies and the application potential in power system operation, Appl. Energy 137 (2015) 511–536.
[40] Z. Hameed, K. Moez, Hybrid forward and backward threshold-compensated RF-DC power converter for RF energy harvesting, IEEE J. Emerg. Sel. Top. Circuits Syst. 4 (3) (2014) 335–343.
[41] X. Li, C.-Y. Tsui, W.-H. Ki, A 13.56 MHz wireless power transfer system with reconfigurable resonant regulating rectifier and wireless power control for implantable medical devices, IEEE J. Solid-State Circuits 50 (4) (2015) 978–989.
[42] H.-M. Lee, M. Ghovanloo, An adaptive reconfigurable active voltage doubler/rectifier for extended-range inductive power transmission, IEEE Trans. Circuits Syst. II Express Briefs 59 (8) (2012) 481–485.
[43] J.-H. Choi, S.-K. Yeo, C.-B. Park, S. Park, J.-S. Lee, G.-H. Cho, A resonant regulating rectifier (3R) operating at 6.78 MHz for a 6W wireless charger with 86% efficiency, in: Solid-State Circuits Conference Digest of Technical Papers (ISSCC), 2013 IEEE International, 2013, pp. 64–65.
[44] H. Jabbar, Y.S. Song, T.T. Jeong, RF energy harvesting system and circuits for charging of mobile devices, IEEE Trans. Consum. Electron. 56 (1) (2010).
[45] M.K. Hosain, A.Z. Kouzani, S. Tye, A. Kaynak, M. Berk, RF rectifiers for EM power harvesting in a deep brain stimulating device, Australas. Phys. Eng. Sci. Med. 38 (1) (2015) 157–172.
[46] N. Van Helleputte, et al., A 345 μW multi-sensor biomedical SoC with bio-impedance, 3-channel ECG, motion artifact reduction, and integrated DSP, IEEE J. Solid-State Circuits 50 (1) (2015) 230–244.
[47] Y. Zhang, et al., A batteryless 19 μW MICS/ISM-band energy harvesting body sensor node SoC for ExG applications, IEEE J. Solid-State Circuits 48 (1) (2013) 199–213.
[48] H. Kim, et al., A configurable and low-power mixed signal SoC for portable ECG monitoring applications, IEEE Trans. Biomed. Circuits Syst. 8 (2) (2014) 257–2267.
[49] L. Yan, J. Bae, S. Lee, T. Roh, K. Song, H.J. Yoo, A 3.9 mW 25-electrode reconfigured sensor for wearable cardiac monitoring system, IEEE J. Solid-State Circuits 46 (1) (2011) 353–364.
[50] R. Muller, et al., A miniaturized 64-channel 225 μW wireless electrocorticographic neural sensor, in: 2014 IEEE International Solid-State Circuits Conference Digest of Technical Papers (ISSCC), 2014, pp. 412–413.
[51] M. Yip, R. Jin, H.H. Nakajima, K.M. Stankovic, A.P. Chandrakasan, A fully-implantable cochlear implant SoC with piezoelectric middle-ear sensor and arbitrary waveform neural stimulation, IEEE J. Solid-State Circuits 50 (1) (2015) 214–229.

Biographies

Le-Giang Tran received his B.S. degree in Biomedical Engineering from HCMC International University, Vietnam in 2014 and M.S. degree in Biomedical Engineering and Biomaterials from Seoul National University of Science and Technology in 2016. For his M.S. research, he worked on developing a wireless power transfer system for biomedical applications. He is currently pursuing Ph.D. degree in Seoul National University of Science and Technology and is focusing on flow sensor for unmanned underwater vehicles and microneedles for intradermal drug delivery.

Hyouk-Kyu Cha received the B.S. and Ph.D. degrees from the Department of Electrical Engineering and Computer Science at Korea Advanced Institute of Science and Technology (KAIST), in Daejeon, Korea, in 2003 and 2009, respectively. From 2009 to 2012, he was with the Institute of Microelectronics (IME), Agency for Science, Technology, and Research (A*STAR), Singapore, as a Scientist where he was involved in the research and development of RF/analog ICs for biomedical applications. Since 2012, he has been with the Department of Electrical and Information Engineering, Seoul National University of Science and Technology (Seoultech), Seoul, Korea, where he is now an Associate Professor. His research interests and areas are analog/RF IC and system design for biomedical devices.

Woo-Tae Park received the B.S. degree in mechanical design from Sungkyunkwan University, Korea, in 2000, the M.S. and Ph.D. degrees in mechanical engineering from Stanford University in 2002 and 2006 respectively. For his Ph.D., he worked on wafer scale encapsulated MEMS devices for biomedical applications. After graduation, he worked at Intel Corporation, Freescale Semiconductor, and IME Singapore, leading several projects on MEMS development. He has authored more than 80 journals and refereed conference papers and has 14 issued and pending patents. He is currently an associate professor at Seoul National University of Science and Technology, conducting research on microscale medical devices.